Haptoglobin polymorphism affects its N-glycosylation pattern in serum

M. Kohansal-Nodehi, M. Swiatek-de Lange *, G. Tabarés, H. Busskamp

Early Development and Reagent Design, Roche Diagnostics GmbH, Penzberg, Germany

A B S T R A C T

Introduction: Haptoglobin (Hp) is an abundant acute-phase protein secreted mainly by the liver into the bloodstream. There are three Hp protein phenotypes (Hp type 1–1, 2–1, and 2–2), which differ in the number of α- and β-chains, type of α-chain (the β-chain type remains the same in all the Hp phenotypes), and the polymers that they form via disulfide bonds. Hp has four N-glycosylation sites on the β-chain. Glycosylation of Hp has been reported frequently as a potential glycobiomarker for many diseases; however, whether Hp polymorphism affects its glycosylation has not yet been addressed extensively or in depth.
Objectives: This study investigated the differences between the glycosylation patterns of Hp phenotypes using serum from 12 healthy individuals (four for each Hp phenotype).
Method: An efficient method for isolating Hp from serum was established and subsequently the Hp phenotype of each sample was characterized by immunoblotting. Then, LC-MS/MS analysis of isolated Hp after treatment with three exoglycosidases (sialidase, α2-3 neuraminidase, Endo F3) was performed to characterize the glycosylation pattern of Hp for each individual sample.
Results: The data reveal significant differences among the branching, sialylation, and fucosylation of Hp types, documenting the effect of Hp polymorphism on its glycosylation.
Conclusion: Overall, the study suggests that Hp phenotype characterization should be considered during the investigation of Hp glycosylation.

Introduction

Haptoglobin (Hp) is an abundant acute-phase protein that is secreted mainly by the liver into the bloodstream [1]. Besides the liver, other organs, including the lungs and skin, are also known to produce Hp to a lesser extent [2,3]. The concentration of Hp in the serum of healthy humans varies between 0.3 and 3 mg/ml, and it is known to be elevated by the occurrence of inflammation [4]. Hp protein consists of at least four chains: two heavy β-chains (∼30–40 kDa each) and two light chains, α1-chain (∼9.1 kDa) and α2-chain (∼16 kDa). The chains are connected via disulfide bridges.

There are two common alleles for Hp, Hp1 and Hp2. Individuals that are homozygotes for Hp1 or Hp2 express type 1–1 or type 2–2 Hp, respectively, whereas heterozygous individuals express type 2–1 [5]. The difference between the Hp types is based on the α-chain type (α1 or α2; β-chain remains identical in all Hp types), and on the number of α and β chains that are connected to each other.

Type 1–1 forms dimers that consist of two α1-chains and two β-chains. Type 2–1 forms linear polymers with various numbers of β-, α1- and α2-chains. Lastly, type 2–2 Hp consists of a varied number of β-chains and exclusively α2-chains that bind to each other with disulfide bridges to make circular polymers (Fig. 1A) [4,5]. The distribution of Hp phenotypes in populations depends on the frequency of Hp1 and Hp2 alleles. In the Western European population, the phenotypic distribution of Hp types 1–1, 2–1 and 2–2 is 15%, 50% and 35%, respectively [6,7]. Among Eastern Asian countries, such as China and Thailand, type 2–2 is prevalent, and in Western African countries, such as Nigeria and Liberia, type 1–1 represents the majority of Hp [7].

Two main functions have been reported for Hp. First, Hp acts as the scavenger for hemoglobin (Hb) during intra and/or extracellular hemolysis. Free Hb in the plasma rapidly binds to Hp with high affinity and low dissociation, and the Hb-Hp complex is rapidly cleared from plasma by monocytes and macrophages [8]. In this way, Hp decreases the oxidative and toxic effect of free Hb in plasma. Type 2–2 Hp is shown to

be less effective as an anti-oxidant compared to type 1–1. This is due to the higher molecular size and circular shape of type 2–2 Hp polymers that decrease its ability to circulate in the extravascular system and capture free Hb [9].

Besides the anti-oxidant role, Hp stimulates angiogenesis, plays a role in several immune response processes, such as activating the innate and adaptive immune response to tissue repair, modulating the proliferation of B-cells, and reducing the severity of autoimmune inflammatory processes [10].

Human Hp is a glycoprotein with four N-glycosylation sites that are located exclusively at the β-chain, resulting in a complex mixture of glyco-proteoforms. The glycosylation sites are located close to each other and in the vicinity of the N-terminus of the β-chain (N184, N207, N211, and N241, Fig. 1C) [11]. The glycan structure of Hp has been explored extensively, mainly by lectin arrays [12,13] and glycan and glycoproteomics analysis methods [11,14,15]. These studies demonstrated the highly sialylated and fucosylated nature of Hp glycan structures. However, although several studies have reported the primary Hp glycan structures, very few are available regarding the effect of the 3D structure of Hp polymers on their glycan structures and how the Hp glycosylation pattern affects its function. The crystal structure of the Hb-Hp complex reveals that the N184 and N207 glycosites are close to the binding interface to Hb [16,17]. Recently, two publications combined native mass spectrometry and binding assays and described the differences in Hp glycosylation in type 1–1 and multimers of type 2–1 and 2–2 and their effect on the binding of Hp to Hb [16,17]. However, both of these studies were performed on the desialylated Hp glyco-proteoforms and did not resolve the differences between glycosites. Another study published by Ivanov et al. [15], applying intact-mass analysis using cross-path reactive chromatography (XP-RC) and MS detection, demonstrated increased fucosylation and a higher number of triantennary structures in Hp 1–1 compared to Hp 2–1. Site-specific glycosylation patterns were not addressed in these studies.

The Hp glycosylation pattern has been reported to be altered in patients with many types of cancers, raising the interest of using it as a protein glycobiomarker for prognostic and diagnostic purposes [1]. For example, an increased level of N-glycan branching, sialylation and/or fucosylation of Hp has been reported for pancreatic [1,18–20], hepatic [11,12,21], lung [22,23], colon [1,21,24] and ovarian [1,25] cancers.

Although the alteration of the site-specific glycosylation pattern of Hp in various diseases has been reported repeatedly before, to the best of our knowledge, very few of these reports [20,26] dealt with the characterization of Hp types in human samples and the variation of glycosylation pattern that might result. By comparing the variation in background glycosylation between the Hp types in control (healthy) samples with that resulting from disease, the sensitivity and specificity of glycobiomarkers might increase, and consequently the number of false-negative and positive hits will be reduced.

Here, we aimed to describe the differences between the glycosylation patterns of Hp phenotypes of healthy individuals to answer how gene polymorphism might affect the Hp glycosylation pattern. To this extent, Hp types were characterized by immunoblotting using an antibody against the Hp α-chains (Fig. 1B). Next, using immunoisolation-LC-MS/MS glycoproteomics workflow (Fig. 1D), the site-specific glycosylation profile of all three types of Hp were described. For the first time, in-depth glycosylation analysis of different Hp types isolated from human serum reveals the significant variation of branching, fucosylation, and sialylation of Hp glycopeptides among the Hp types. Our data suggest the significant effect of polymorphism on glycosylation of Hp, which needs to be considered in Hp biomarker discovery studies in order to obtain more accurate and reliable data

Materials and methods

Reagents and materials

Streptavidin-coated magnetic particles (Ref. 11,641,786,001), Endoproteinase Glu-C (Ref. 11047817001), and the F(ab́)2 antibody
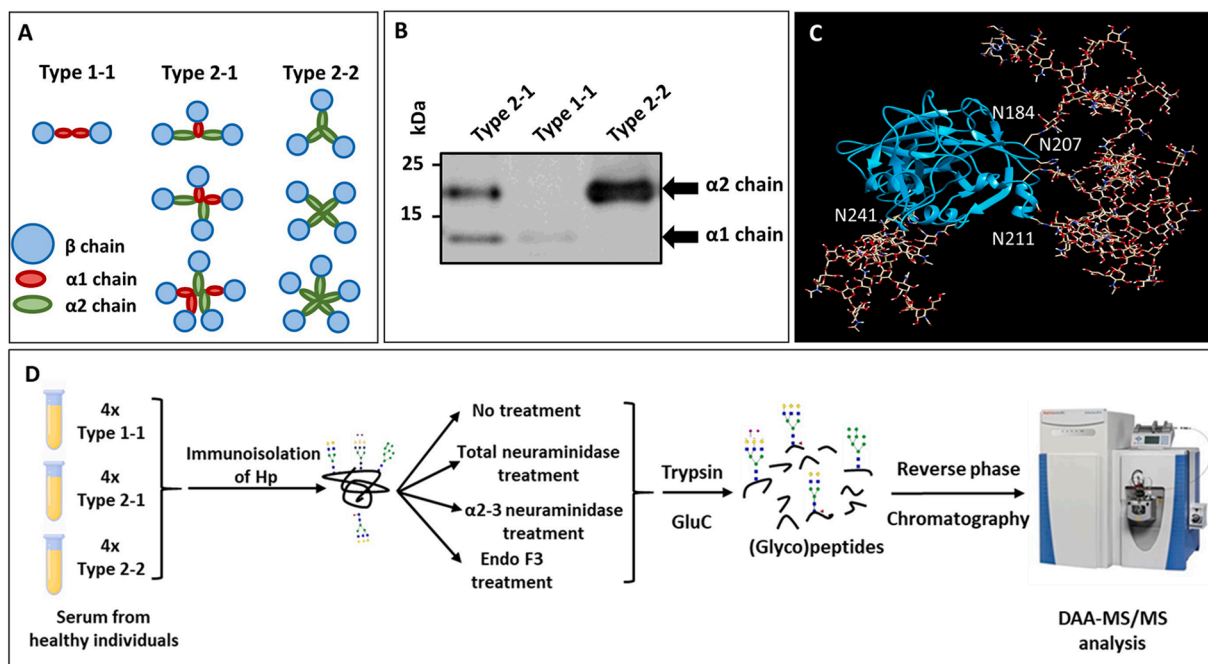

Fig. 1. Haptoglobin polymorphism, glycosylation, and experimental design. Haptoglobin (Hp) has three phenotypes based on the number of α- and β-chains, type of α-chain (the β-chains type remain the same in all the Hp types), and type of polymers that they form via disulfide bonds. Type 1–1 exclusively binds as a dimer with α1- and β-chains. Type 2–1 forms linear polymers consisting of α1-, α2-, and β-chains. Type 2–2 forms circular polymers, with α2- and β-chains (A) [4,5]. Hp type can be characterized using denaturing SDS-PAGE and immunoblotting (B). Hp has four N-glycosylation sites on the β-chain (β-chain shown in cyan color), at N184, N207, N211 and N241 (C) [11]. Hp immunoprecipitation from human sera, exoglycosidase treatment followed by glycoproteomics: workflow used for in-depth characterization of Hp glycosylation (D). (For interpretation of the references to color in this figure legend, the reader is referred to the web version of this article.)

fragment conjugated with biotin (MAK < Haptoglobin > M−1.1.13-F (ab′)2-Bi(DDS,Sux) were obtained from Roche Diagnostics GmbH (Mannheim, Germany). Phosphate buffered saline (PBS), Tween 20, iodoacetamide (IAM), and ammonium bicarbonate (ABC) were purchased from Sigma-Aldrich (St. Louis, USA). Acetonitrile (ACN) and formic acid (FA), both UPLC/MS grade, were purchased from Biosolve (Dieuze, France). NuPAGE 4–12% Bis-Tris protein gels, NuPAGE MOPS SDS running buffer, PVDF blotting membranes, NuPAGE™ transfer buffer, NuPAGE LDS sample buffer, Pierce ECL western blotting substrate kit, and dithiothreitol (DTT) were purchased from Thermo Fisher Scientific (Rockford, USA). LowCross blocking buffer was obtained from Candor (Wangen, Germany). Mouse antibodies against Hp α-chain and secondary HRP-conjugated rabbit anti-mouse IgG were obtained from Abcam (Waltham, USA). Glyko Sialidase A, α2-3 neuraminidase, and Endo F3 were purchased from Prozyme (GK80040), New England Biolab, (P0743S), and QA bio (E-EF03), respectively. Sodium chloride (NaCl), potassium chloride (KCl), Tris Base, glycine, and sodium hydroxide solution were purchased from Merck (Darmstadt, Germany). The remaining chemicals and reagents were purchased from the following suppliers: sequencing grade modified trypsin (Promega, Madison, WI), Nanosep® Centrifugal Devices with Omega™ Membrane −10 K (PALL, US).

Buffers

TBST: 20 mM Tris, 150 mM NaCl, 0.1% Tween 20, pH 7.4; PBS: 10 mM phosphate buffer, 2.7 mM KCl, 137 mM NaCl, pH 7.4; PBST: 0.1% Tween 20 in PBS buffer; Elution buffer: 0.2 M Glycin, pH 2.6; Endo F3 treatment buffer: 50 mM sodium acetate, pH 4.5; Total neuraminidase (Sialidase) treatment buffer: 50 mM sodium phosphate, pH 6.0; α2-3 neuraminidase treatment buffer: 50 mM sodium citrate, pH 6.0; ABC buffer: ammonium bicarbonate (ABC), 50 mM; Denaturing buffer: 1 mg/ml PPS (3-[3-(1,1-Bisheptyloxyethyl)pyridin-1-yl]propan-1-sulfonat) in 50 mM ABC.

Human serum samples

Blood samples were obtained from 12 healthy individuals (four type 1–1, four type 2–1, and four type 2–2) following the standard operating procedure. Collection of samples was approved by the Roche ethics committee. Informed written consent was obtained from all subjects who donated blood. Donors were age-matched and had a mean age of 31 years (range: 22 to 39 years). With regard to gender, 30% of donors were women and 70% men.

Serum sample preparation

Serum samples were drawn into a serum tube and allowed to clot for at least 60 min and up to 120 min at room temperature (RT). After centrifugation (10 min, 2000g), the supernatant was divided into 1 ml aliquots and frozen at −70 °C. After preparation, the samples were stored at −70 °C until time of analysis, and repeated freezing and thawing of samples was avoided.

Immunoblotting

In order to characterize the Hp type of the samples, the presence and molecular size of the α-chains were examined by immunoblotting. Two microliters of serum samples were diluted 25 times with 2X sample buffer and 25 mM DTT and heated for 10 min at 70 °C to denature the proteins and reduce the disulfide bonds. Ten microliters of each sample were used for analysis on SDS-PAGE gels. The proteins separated on the gel were transferred to a PVDF membrane according to standard procedures [27]. Membranes were blocked for 30 min with LowCross buffer at RT. The membrane was incubated with the primary antibody against Hp α-chains at a dilution of 1:500 overnight at 4 °C. Membranes were

washed three times with TBST buffer for 10 min at RT and incubated with HRP-conjugated mouse antibody at a dilution of 1:1000 for 1 h at RT. Membranes were washed three more times with TBST and the immunoreactive proteins were developed with enhanced chemiluminescence reagent. Signals were detected with a LAS-1000 imaging system.

Hp immunoprecipitation from serum

In order to isolate Hp from serum, streptavidin beads (10 mg) were incubated on the rotator for 1 h at RT with 150 µg of in-house biotin-labeled F(ab′)2 fragment (diluted in 1 ml PBS) against the Hp β chain. The excess of F(ab′)2 fragments was washed three times with PBS. In a separate vial, 50 µl of serum was incubated with 5 µl of 20 mM DTT at 37 °C for 1 h. Then samples were treated with 10 µl of 50 mM IAM at RT for 30 min. Samples were diluted up to 2 ml with PBS and were added to antibody-coated beads and incubated for 2 h at RT on a rotator. Then, the unbound proteins were removed from the beads by washing twice with 1 ml PBST buffer and twice with 1 ml PBS buffer. Next, the Hp-bound fraction was eluted from the beads by 500 µl glycine buffer (pH: 2.6) in two steps. After each elution step, 200 µl NaOH (1 N) was added to the eluted fraction to neutralize the pH.

Glycosidase treatments

The eluted Hp fraction from each sample was further divided into four fractions, three to be treated with glycosidases and one fraction to be kept as control (no treatment). Each fraction was loaded onto a Nanosep filter (cut off: 10 kDa) and centrifuged at 10 K g for 20 min to dry the filter. The filter was washed once with 250 µl of the appropriate glycosidase buffer (see the 'Buffers' section of the Material and Methods) depending on glycosidase treatment. Then 47 µl of the same buffer was added to the filter followed by 3 µl of glycosidases (either sialidase, α2-3 neuraminidase, or Endo F3); in the control condition, 3 µl of buffer was added. Samples were incubated overnight at 37 °C. The next day, filters were dried by one-step centrifugation at 10 K g for 20 min. Samples were then used for the filter-aided sample preparation (FASP) digestion.

FASP digestion

For the FASP digestion, filters were washed once with 100 µl of denaturing buffer. Filters were dried by centrifugation at 10 K g for 20 min. Then 50 µl of denaturing buffer and 5 µl of DTT (10 mM) were added to the samples and incubated for 30 min at 50 °C. The samples were left to cool down at RT for 10 min and were incubated with 5 µl of IAM (55 mM) for 30 min at 37 °C in the dark. Samples were centrifuged at 10 K g for 20 min to wash out the buffer. Filters were washed again once with 100 µl of ABC buffer. Then in the first endoprotease step, 6 µg of trypsin and 50 µl of ABC buffer were added to filters and incubated for 3 h at 37 °C. On the next endoprotease treatment step, 10 µg of GluC were added to the samples. Samples were incubated overnight at 25 °C. The next day, the digested peptides were eluted from the membrane by one-step centrifugation at 10 K g for 20 min.

LC-MS/MS analysis

For LC-MS/MS analysis, an HF-X mass spectrometer (Thermo Fisher Scientific, Germany) coupled to a Vanquish (Thermo Fisher Scientific, Germany) UHPLC system was used. Twenty microliters of the eluted peptides from the previous step were injected into the LC-MS system. Peptides were separated on a C18 column (Waters, XSelect CSH C18 Column, 130 Å, 3.5 µm, 2.1 mm X 150 mm), incubated at 50 °C in a binary solvent gradient composed of H_2O containing 0.1% formic acid (eluent A) and acetonitrile containing 0.1% formic acid (eluent B) with a flow rate of 320 µl/min. The LC gradient was set as follows: 0%−30% B (0–30 min), 30%−80% B (30–31 min), 80% B (31–36 min), 80%-0% B

(36–37 min), and 0% B (37–42 min). Separated peptides were ionized by electrospray ionization (ESI) source and analyzed on the positive ion and the data-dependent acquisition mode. Full scan MS spectra were acquired in the range of 300–2000 *m/z* at a resolution of 60,000, 10e⁶ automatic gain control (AGC), 50 ms injection time. The top five most intense peaks from the survey scan were selected for fragmentation with Higher-energy Collisional Dissociation (HCD), at the normalized collision energy of 28, resolution of 15000, 1e⁵ AGC, and 150 ms injection time. A representative MS/MS spectra of glycopeptides from each of the four glycosites and glycan assignment to the fragments' peaks is depicted in Fig. S1.

Data analysis

Acquired MS spectra were processed with the Byonic (Protein Metrics, CA, US) search engine embedded in Proteome Discoverer 2.2 (Thermo Fisher Scientific) against the Uniprot haptoglobin protein sequence (P00738) and a combination of curated Byonic glycan databases that consisted of 309 mammalian N-glycans with no sodium, 57 human plasma N-glycans and 182 human N-glycans without multiple fucose. The Byonic/Proteome Discoverer search was configured as follows: the mass tolerance was set to 10 and 20 ppm for precursor and fragment searches, respectively. Trypsin and GluC were set as proteases with a maximum of two missed cleavages allowed. Carbamidomethylation of cysteine was set as a fixed modification, and methionine oxidation and glycosylation on asparagine were specified as variable modifications. Results were filtered at a 1% false discovery rate (FDR) and a confidence threshold of the Byonic score greater than 100. In text format, glycans are described as follows: HexNAc(x)Hex(x)Fuc(x)NeuAc (x), where HexNAc, Hex, Fuc, and NeuAc represent N-acetylglucos (galactose)amine, mannose (glucose, galactose), fucose and N-acetylneuraminic acid, respectively. The numbers in the parentheses represent the number of monomers in the glycans. Schematic representations are according to the Symbol Nomenclature For Glycans (SNFG) hosted by NCBI, National Center for Biotechnology Information [28,29].

Automated quantitative analysis was performed by Proteome Discoverer. The peak area of glycopeptides was automatically integrated and used as the relative quantitative values. The glycopeptides peak area values in each sample were normalized to the average Hp protein level (from MS data) in all samples to make sure that observed differences are due to different Hp types and not different Hp concentrations in the samples. In order to investigate the difference among glycan characteristics, such as fucosylation, sialylation, and branching, the abundance of the glycopeptides with the same characteristics was summed and reported as the cumulative intensity of glycopeptides.

The data were processed by Byonic/Proteome Discoverer and exported as excel files for downstream analysis. For the determination of significant differences between the glycosylation patterns of each Hp type, a two-tailed, equal variance standard *t*-test was used. A p-value lower than 0.05 was considered a significant difference.

The GlycoWorkbench package was used for visualization of the glycans, [30], and the Hp structure (PDB ID: 4WJG, [3130]) from the protein data bank and GlyProt tool was used to model the glycans on the crystal structure of Hp [32]. For the visualization and calculation of r-squared of the correlation charts among the samples, Perseus software was used [33].

Results

This study investigated whether the Hp polymorphism in the healthy population affects its N-glycosylation pattern. To answer this question, first, the Hp types of healthy individual donors were characterized by immunoblotting. Type 1–1 only has α1 chain; type 2–2 only has α2 chains, and type 2–1 has both α1 and α2 chains. α1 and α2 chains have a very similar protein sequence. However, α2 has a sequence repetition;

therefore, it has a larger molecular size (~16 kDa) than the α1 chain (~9.1 kDa). This enabled us to separate α chains on a denaturing SDS-PAGE and distinguished them by immunoblotting using an antibody against the α-chain. Fig. 1B shows a representative immunoblotted membrane, in which the presence of both α1- and α2-chains demonstrates Hp type 2–1 and exclusive presence of α1- or α2-chains represent type 1–1 and type 2–2, respectively.

In the next step, in order to enrich the Hp, Hp protein was immunoisolated from donors' sera using streptavidin beads coated with a biotinylated antibody against the Hp β-chain. The Hp isolated from each donor was divided into four aliquots. Each aliquot was treated in the following four conditions: (1) Total sialidase treatment was used to cut all sialic acids with different linkages, thereby decreasing the heterogeneity of glycoforms. This treatment was used to investigate the branching of glycopeptides; (2) α2-3 neuraminidase treatment was used to study the linkage of sialic acids; (3) Endo F3 treatment was applied to study the localization of fucose (core or antennary) on the glycoforms; and finally, (4) one fraction was kept without any treatment to study sialylation and fucosylation, and as reference for other conditions (Fig. 1D). Then, the isolated Hp protein was digested to peptides using trypsin and GluC proteases to leave only one glycosylation site in each peptide. This enabled us to compare the glycosylation pattern of single glycosites separately between Hp types. To assess the reproducibility of the biological replicates, the Pearson correlation coefficients between intensities of glycopeptides in biological replicates of "no treatment" conditions were determined (Fig. S2). High correlation between the replicates was confirmed, with the coefficients greater than 0.72. A control sample (a mix of all cohort samples) was prepared and measured separately at the beginning and the end of the sample measurement workflow. We observed a coefficient of variation (CV) of 11.3% for the Hp protein level and 12.1% for the top three peptide level along the measurement workflow for all samples, demonstrating high method reproducibility.

Branching

In order to study the branching of glycan trees on different Hp glycosites and among different Hp types, glycopeptides were grouped into three categories: bi-, tri-, or tetraantennary, regardless of the presence of fucose or sialic acids. The combined pattern of all the glycosites revealed a significant difference in tetraantennary glycopeptides that are higher in Hp type 1–1 compared to type 2–1 and 2–2 (Fig. S3A).

In the individual analyses of each glycosite, at N241 glycosite, tri- and tetraantennary glycopeptides in type 2–2 Hp were significantly lower compared to type 1–1 and 2–1 Hp. Unlike the N241 site, at N184 glycosite, the tri- and tetraantennary glycopeptides were significantly higher for type 2–2 compared to type 1–1 and type 2–1 (Fig. 2A and 2D). Since both tri- and tetraantennary are bulky glycoforms, this finding hints that N184 might have more flexibility compared to N241 in circular polymers of Hp type 2–2.

At the N207 glycosite, tri-, and even biantennary glycans were less frequently detected in Hp type 2–2 compared to type 1–1 and 2–1. Finally, at the N211 position, which is very close to N207, the biantennary glycans are more frequently present in type 2–2 compared to type 1–1 and 2–1, but vice versa for the tri- and tetraantennary glycans (Fig. 2B and 2C). Overall, these observations demonstrate that steric hindrance might prevent the mid-sequence glycosites (N207 and N211) from being occupied by hyper-branched, bulky glycoforms, especially in type 2–2 circular polymers.

Sialylation

To investigate sialylation among the Hp types, the mono-, bi-, and trisialylated glycopeptides were grouped together, regardless of their branching or fucosylation. N184 and N241 demonstrated most of the significant differences between the Hp types, where bi- and trisialylated
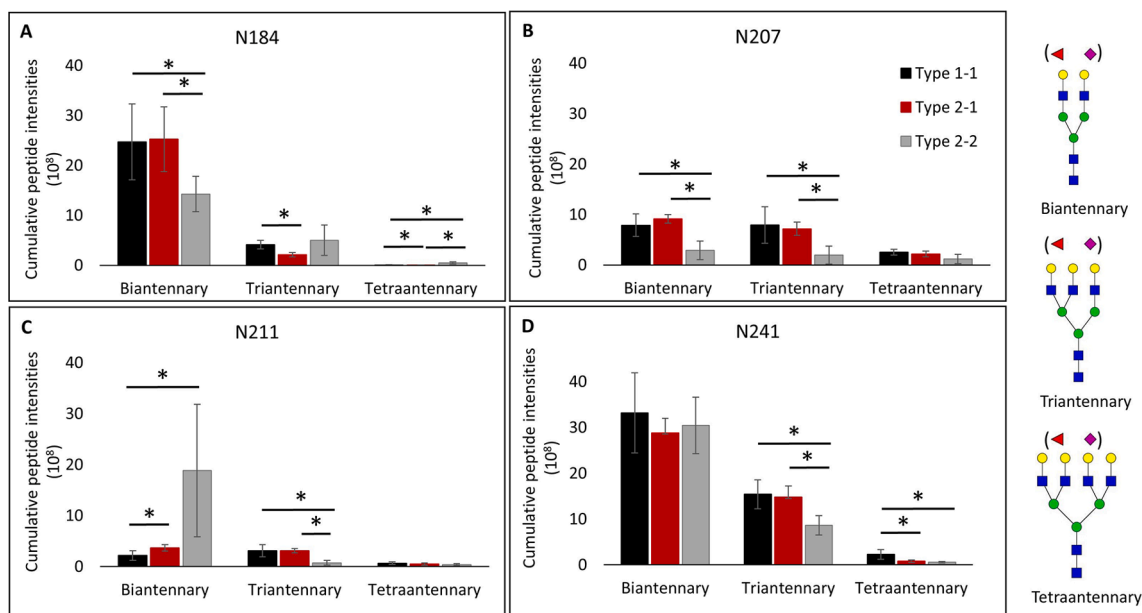
Fig. 2. Branching of glycopeptides is significantly different among Hp types. Glycopeptides were grouped based on the number of branches, regardless of their fucosylation and sialylation status. The branching was analyzed separately for each glycosylation site: N184 (A), N207 (B), N211 (C), and N241 (D). On all the glycosites except N184, multi-branched glycans (tri- and tetra antennary) are less often present in type 2–2 compared to type 1–1. The biantennary glycans are significantly lower at N184 and N207 in type 2–2, in contrast to N211 which shows higher biantennary glycans for type 2–2 compared to other types, and to N241 which shows no significant difference (*p-value < 0.05, using student *t*-test). Right-hand-side: schematic representation of bi-, tri-, and tetraantennary glycans according to Symbol Nomenclature For Glycans (SNFG) hosted by NCBI, National Center for Biotechnology Information.

glycopeptides were significantly lower in type 2–2 compared to type 1–1 and type 2–1, and monosialylated glycans were slightly higher in type 2–2 (N184) or showed no significant difference among Hp types (N241). This observation is very much in line with previous reports in which type 2–2 shows fewer trisialylated glycans [26]. Since sialic acid monomers are negatively charged, this could be evidence for more electrostatic hindrance in type 2–2 polymers at the N184 position compared to the other types of Hp (Fig. 3A and 3D). N207 and N211 have a similar pattern of sialylation. At these two sites, bisialylated glycans were present significantly more in type 2–2 compared to other types of Hp (Fig. 3B and 3C). When the sialylation of all glycosites were considered together, we did not observe any significant changes among the Hp types (Fig. S3B).

Besides the overall sialylation, one of the characteristics of glycoproteins that is known to be modulated in different disease conditions is the linkage of sialic acids. Therefore, it was decided to investigate if the phenotype of Hp also affects the linkage of sialic acids on the N-glycan trees. To this end, the isolated Hp was treated with α2-3 neuraminidase. This enzyme specifically cuts the sialic acids that are linked to carbon 3 of their neighboring monomers and leaves the sialic acids with other kinds of linkages intact (Fig. 4A). First, a comparison was made in the number of glycopeptides that were significantly differentially regulated in the Hp types after treatment with α2-3 neuraminidase. It was observed that type 1–1 had 12 and 18 glycopeptides that were significantly different compared to type 2–1 and type 2–2, respectively. In contrast, only one glycopeptide showed a significant difference between type 2–1 and type 2–2 (Fig. 4B). This observation documents that the sialic acid linkages have a similar pattern in type 2–1 and 2–2, whereas type 1–1 shows more differences from the other Hp types.

Then the sialylated glycopeptides were grouped based on the number of sialic acids to compare the intensity of sialylated glycans before and after treatment with α2-3 neuraminidase. This comparison demonstrated that the intensity of trisialylated glycans was decreased after treatment with α2-3 neuraminidase in all Hp types, whereas, the intensity of bi-, mono- and non-sialylated glycans was increased, showing that most α2-3-linked sialic acids are present in trisialylated glycans in

all three Hp types (Fig. 4C). This is very much in line with the previous observation that α-2,3-sialyltransferase prefers multi-branched rather than bi- or mono-branched glycans as a substrate [34].

Next the study examined which glycopeptides are differentially regulated after treatment with α2-3 neuraminidase for each of the Hp types, grouped according to the number of sialic acids. This analysis highlighted the following observations: first, in type 1–1, more sialylated glycans are differentially regulated after α2-3 neuraminidase treatment compared to the other two types; second, in all types, the intensity of trisialylated glycopeptides is decreased after treatment. In contrast, bi-, mono-, and non-sialylated glycopeptides showed an increase in their intensity, supporting the fact that α2-3-linked sialic acids are more often present in trisialylated glycopeptides (Fig. 4D-F); third, in type 2–2, most of the trisialylated glycans are converted to bisialylated glycans after the α2-3 neuraminidase treatment, showing that only one of the three sialic acids was α2-3-linked (Fig. 4F). However, in type 1–1 and 2–1, the majority of trisialylated glycans were converted to monosialylated glycans, showing that two of the sialic acids were α2-3 linked (Fig. 4D and 4E).

The analysis was then limited to the samples that were treated with α2-3 neuraminidase to analyze the sialylated glycoforms that contain sialic acids with α2-6 linkage. The mono-, bi-, tri-sialylated glycopeptides were grouped together, regardless of their branching or fucosylation (Fig. S4). Interestingly, it was observed that removing α2-3-linked sialic acid decreases the significant differences among Hp types, specifically at N184 and N241. In addition, a decrease in bisialylated glycans was observed at N207 and N211 (compare Fig. 3 and Fig. S4).

Finally, the summed sialylation level was compared between the three types of Hp, notwithstanding glycosite position. Although significant differences in sialylation were observed when considering the sites separately, this effect was not reproduced in the cumulative analysis (Fig. S3B). This observation is in line with the results presented for Hp 1–1 and 2–1 by Ivanov et al. 2022 [15].
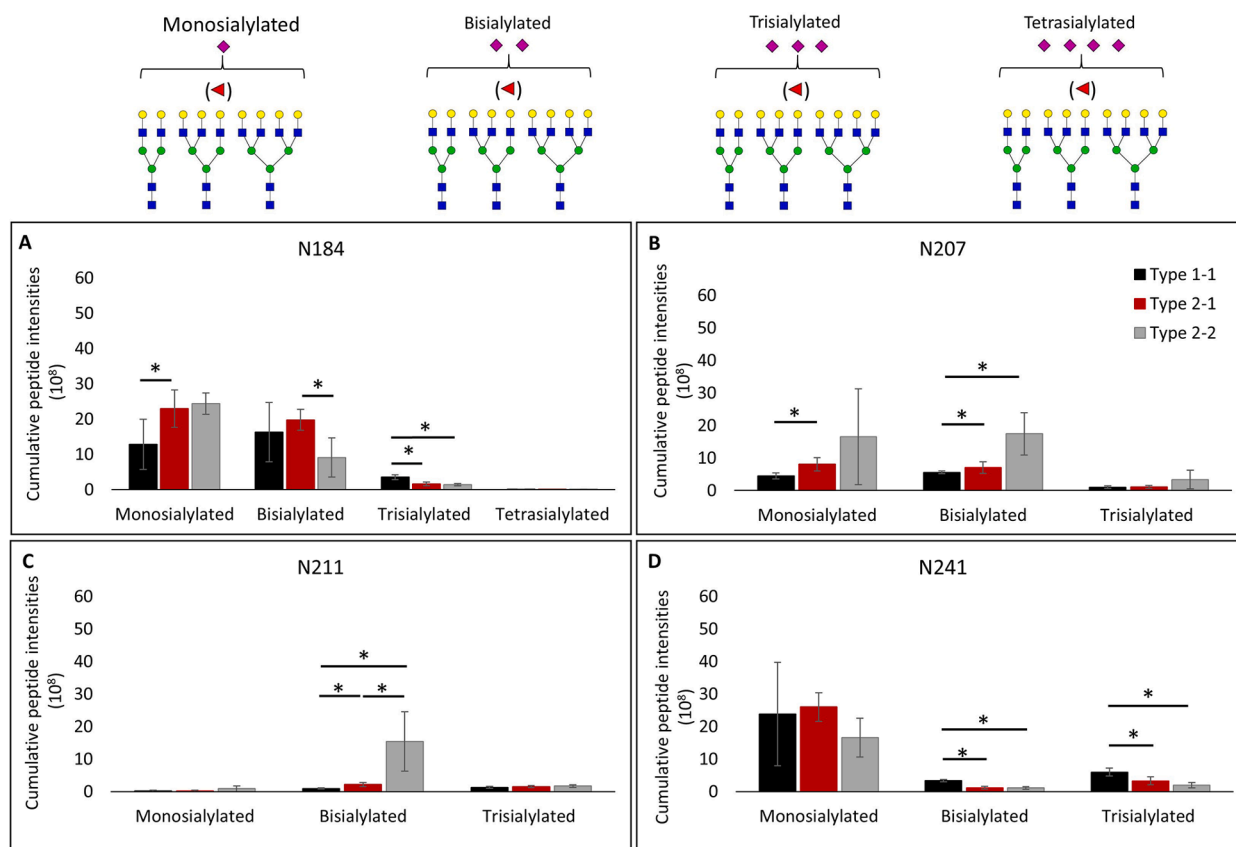
Fig. 3. Sialylation of glycopeptides is significantly different among Hp types. Glycopeptides were grouped based on the number of sialic acids, regardless of their fucosylation and branching status. The sialylation was analyzed separately for each glycosylation site: N184 (A), N207 (B), N211 (C), and N241 (D). Most of the differences among Hp type were observed at N184 and N241, where bi- and trisialylated glycopeptides were significantly lower in type 2–2 compared to type 1–1 and type 2–1, documenting the possible electro- and steric-hindrance at the N184 position in the 2–2 Hp polymers (*p-value < 0.05, using student *t*-test). Upper panel: schematic representation of bi-, tri-, and tetraantennary glycans according to Symbol Nomenclature For Glycans (SNFG) hosted by NCBI, National Center for Biotechnology Information.

Fucosylation

To compare the fucosylation status of Hp among different types, the mono-, di, and trifucosylated glycopeptides were grouped, regardless of branching and sialylation. At all glycosites, levels of monofucosylated glycosites were significantly higher in type 1–1 compared to type 2–1 and 2–2 (Fig. S3C). These results agree with differences in fucosylation levels between Hp 1–1 and 2–1 described previously by Ivanov et al. [15], but are contradictory to the lectin- and antibody-based fucosylation studies performed by Morishita et al. [20].

Analyzing glycosites separately, it was observed that N207 and N211, the two middle glycosites that are located very close to each other, are fucosylated to a much lesser extent compared to N184 and N241, demonstrating that fucosylation introduces considerable steric hindrance at these two sites or that fucosyltransferases have difficulty accessing the Hp middle glycosites. However, all three Hp types showed a similar pattern in this regard.

Another observation was that most of the fucosylated glycans are bifucosylated (combinations of core- and arm-fucoses), especially at N184 and N241, which is similar among the Hp types. However, type 2–2 is less mono- and bifucosylated at N241 compared to type 1–1 (Fig. 5D). In the case of N184, only monofucosylated glycans showed a significant difference among Hp types (Fig. 5A), again supporting that N184 is more flexible to bind bulky glycans compared to other glycosites or that there is better accessibility for fucosyltransferases at N184.

Since the localization of fucose in Hp glycosites is one of the parameters that has been reported to be altered in different disease conditions, Hp protein was then treated with Endo F3 enzyme. Endo F3

cleaves the glycosidic bond between the first and second N-acetylglucosamine in the glycan core of bi- and triantenna glycans only if the fucose monomer is present (Fig. 5E). The product of this enzymatic reaction is a dimer of N-acetylglucosamine and fucose at the glycosites. Thus, in order to investigate if the core-fucosylation pattern is different between Hp types, the intensity of the glycopeptides was compared with N-acetylglucosamine and fucose (HexNAc(1)Fuc(1)). The analysis revealed no significant differences in the intensity of the HexNAc(1)Fuc(1) glycopeptides, and therefore in core fucosylation, between the Hp types (Fig. 5E).

Discussion

To date, the effect of genetic polymorphism on protein glycosylation has been poorly investigated. This is especially important for glycoproteins that are considered as biomarkers or therapeutic targets and can lead to the discovery of personalized biomarkers that are based on the genotype of individuals. Recently, in two publications [16,35], the effect of gene polymorphism on the glyco-proteoforms of fetuin and Hp has been studied. In the case of fetuin, the study suggested that the differences in glycosylation due to polymorphism should be considered if fetuin glycosylation is used as a biomarker for sepsis [26].

Here, we combined characterization of Hp types with peptide-centric glycoproteomics of isolated Hp protein from healthy donors' sera to analyze the effect of Hp polymorphism on its glycosylation. Age, gender and underlying diseases are known to change protein glycosylation patterns [21]. To minimize such pre-analytical effects, we collected samples from age-matched healthy donors. Our data demonstrate that
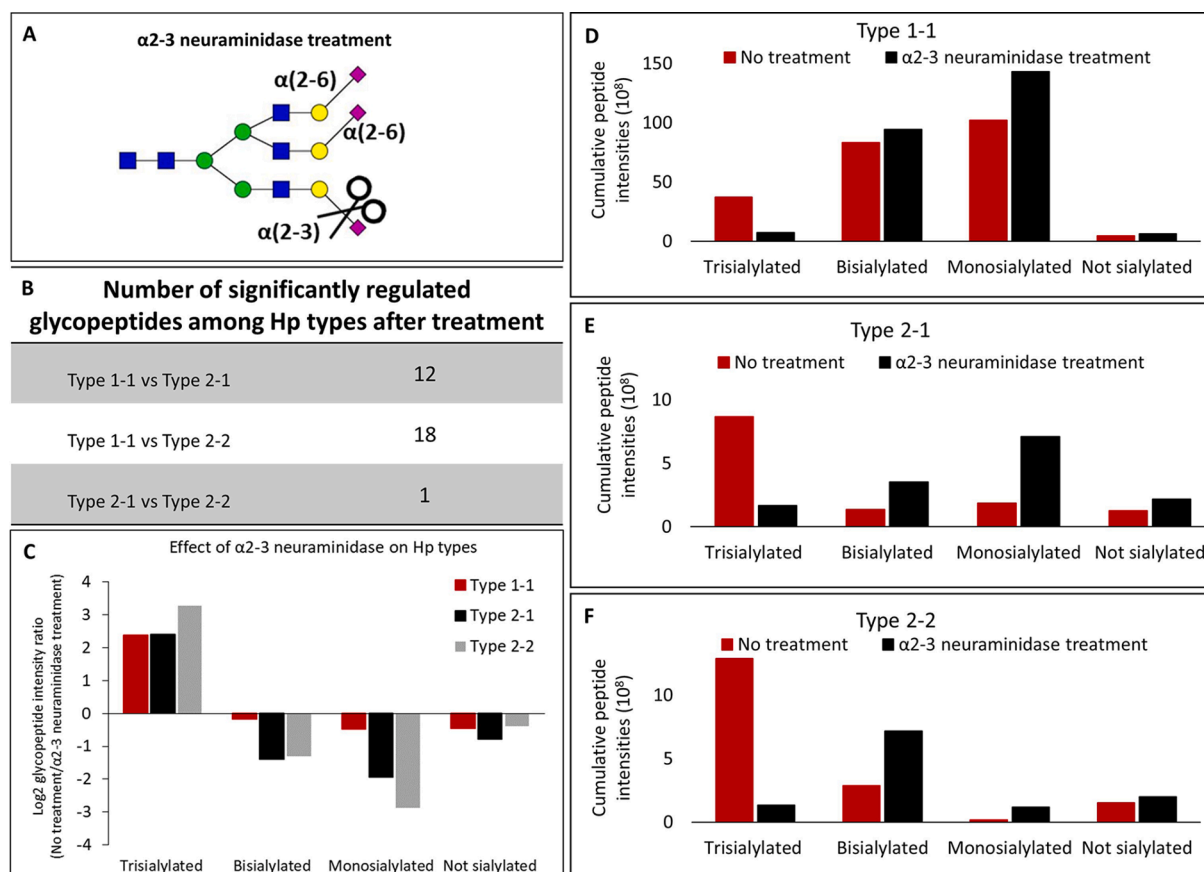
Fig. 4. Sialic acid linkage of Hp type 1–1 glycopeptides shows differences from type 2–1 and 2–2. Isolated serum Hp was treated with α2-3 neuraminidase, which specifically cut sialic acids that are bound to the rest of the Gal-residues with 2–3 linkage, the rest of the sialic acids remain intact (A). Comparison of the intensity of glycopeptides after α2-3 neuraminidase treatment revealed 12 and 18 glycopeptides that have significant differences in type 1–1 compared with type 2–1 and 2–2, respectively. Type 2–1 and 2–2 show high similarity in the linkage of sialic acid with only one glycosite with significantly different intensity after treatment with α2-3 neuraminidase (B). Log2 ratio of glycopeptides before and after treatment with α2-3 neuraminidase is calculated. Treatment resulting in a decrease of sialylated glycan will have positive values, and vice versa. Treatment with α2-3 neuraminidase decreases abundance of trisialylated glycopeptides and increases bi-, mono, and non-sialylated glycans, mostly in type 2–1 and 2–2 and to a lesser extent in type 1–1 (C). Distribution and abundance of glycans containing different numbers of sialic acids alters among Hp types after treatment with α2-3 neuraminidase (D-F).

samples derived from donors with different Hp phenotypes have significant differences in their glycosylation patterns. We further investigated, in detail, parameters of glycosylation that are altered in different Hp types, such as branching, sialylation, and fucosylation. It is well documented that Hp monomers combine as dimers (in type 1–1) and polymers (in types 2–1 and 2–2) that are connected to each other via the disulfide bonds of α1- and α2-chains [36]. In contrast, β-chains, in which glycosylation sites are located, are identical in all Hp types. Since Hp polymerization and glycosylation occurs in the cell [37], we speculate that the different 3D shape and size of polymers among the Hp types may affect glycosylation, either by decreasing the flexibility of glycosites to accommodate the bulky glycans or by restricting the accessibility of the Hp glycan structure to the glycosyltransferases.

Based on the resolved crystal structure [31] of the Hp 1–1 dimer, glycosites in one Hp monomer are close to each other, especially N207 and N211. This can explain why less highly branched and fucosylated glycans (most probably due to steric hindrance) are observed in both N207 and N211 in all Hp types. Moreover, the glycosites of one monomer are further apart from sites of the other monomer in type 1–1 Hp dimers compared to polymers in type 2–1 and 2–2 (Fig. 6A). Based on the available crystal structure of Hp type 1–1 we modeled the structure of linear polymers of type 2–1, and the circular polymers of type 2–2: once with biantennary glycans and once with tetraantennary glycans (Fig. 6A and 6B). The linear structure of type 2–1 polymers would provide more space for bulky multi-branched glycans compared to the

circular polymers of the Hp type 2–2. This could explain our observation that type 2–2 has fewer branched glycans compared to type 2–1.

On the other hand, it is known that the addition of sialic acids largely decreases the flexibility of glycans [38]. Therefore, it is possible that the presence of fewer sialylated glycans in type 2–2, compared to 2–1 and 1–1, provides the flexibility that is needed to form the circular polymers. Notably, N241, which in the Hp monomer seems to be further apart from the other glycosites, seems to clash with the glycans of other Hp monomers when forming both circular and linear polymers, consequently introducing electro and steric hindrance.

In our data, we observed that the middle glycosites (N207 and N211) of Hp are fucosylated to a much lesser extent compared to the other sites. Since fucosylation is one of the last steps in the process of protein glycosylation in the Golgi system [39], where proteins are folded almost completely, the structure of folded proteins might decrease the accessibility of fucosyltransferases to these two middle sites.

One of the main functions of Hp is to bind to free Hb and clear it from the blood to decrease its oxidative toxicity [40]. Type 2–2 Hp is reported to be less efficient as a scavenger of Hb [41], and it is also known that the structure of glycans can affect its binding to Hb. Specifically, branching would destabilize the binding of Hp to Hb, while fucosylation increases the Hb-binding ability of Hp. It has also been shown that N184 and N207 are the closest glycosites to the Hb-binding site [17]. In our data, the N184 glycosite showed the most significant difference between Hp types. We observed more multi-branched and lower fucosylated glycans
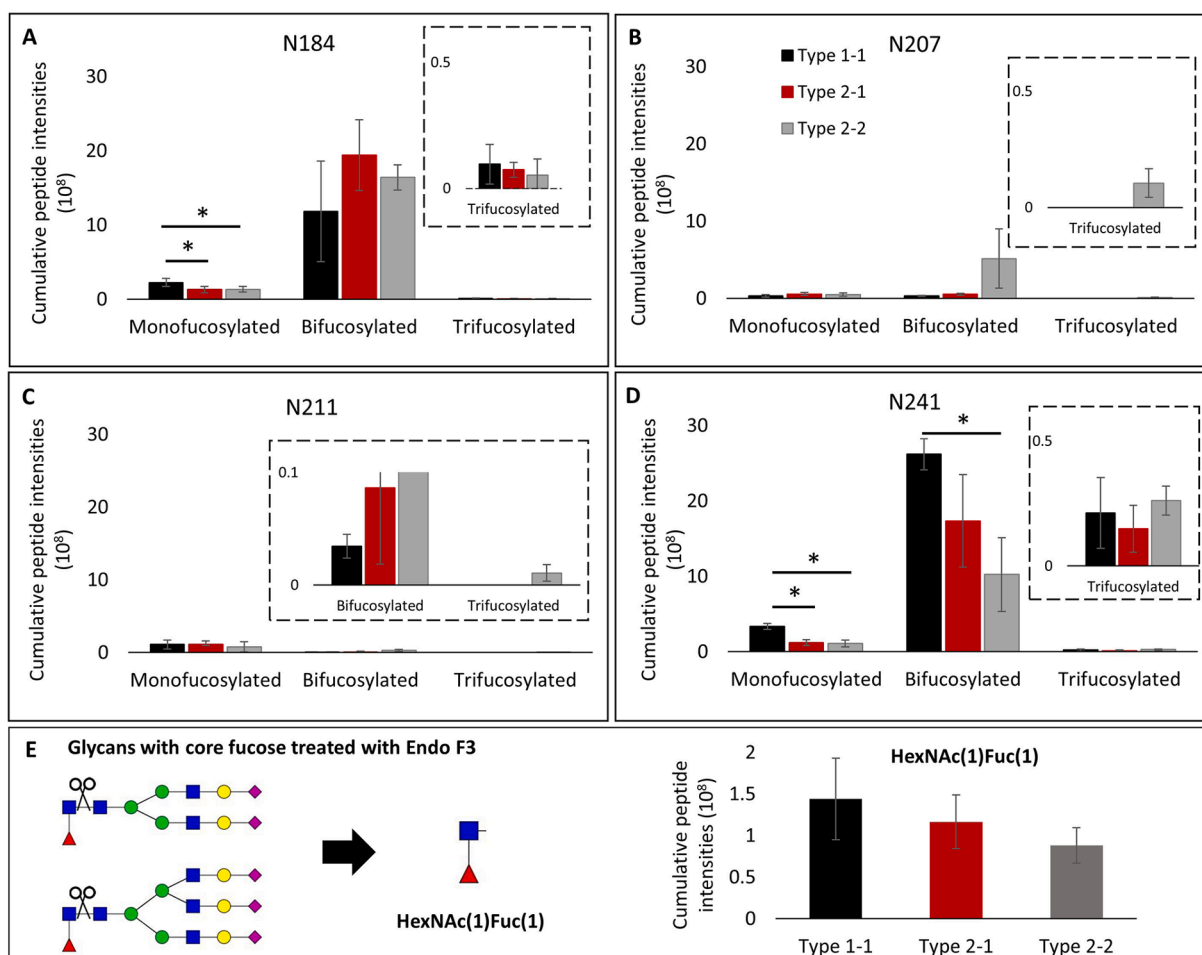
Fig. 5. Differences among fucosylation of glycopeptides between Hp types. Glycopeptides were grouped based on the number of fucose monomers, regardless of their sialylation and branching status. Fucosylation was analyzed separately for the glycosylation sites: N184 (A), N207 (B, insert with different y-scale), N211 (C, insert with different y-scale), and N241 (D). Among glycosites, N184 and N241 were more fucosylated, specifically bifucosylated. At both sites type 1–1 is also more monofucosylated compared to type 2–1 and 2–2 (A and D). Isolated Hp was treated with Endo F3 to investigate the localization of core fucose. Endo F3 cuts the glycosidic bond between two N-acetylglucosmines at the core of the glycan tree. The remaining product is a dimer of N-acetylglucosmine (HexNAc) and core fucose (Fuc). The comparison of glycopeptides with the HexNAc(1)Fuc(1) dimer between the Hp types did not reveal any significant difference, suggesting that the localization of core fucose is not affected by the type of Hp (E). Bars that are empty/absent (zero) indicate that the glycan species was not detected in that Hp type in this study.

at N184 in Hp type 2–2 compared to the other types. Therefore, it can be hypothesized that the lower efficiency of binding to Hb in type 2–2 Hp could be due to the difference in Hp glycosylation pattern (multi-branching and low fucosylation) at N184.

Cumulative analyses of the glycosylation patterns for each Hp type revealed significantly higher levels of monofucosylation and tetraan-tennary structures in Hp 1–1 compared to Hp types 2–1 and 2–2. This agrees with previous observations by Ivanov et al. [15]. Interestingly, the fucosylation data generated with MS-based methods is contradictory to the results obtained with lectin- or antibody-based assays [20]. In that publication, Morishita et al., demonstrated the lowest fucosylation level for Hp 1–1 compared to other types [20]. This discrepancy could be explained by the steric hindrance of the antibody or lectin binding to the Hp 1–1 or by the decreased avidity of the reagents to the dimeric Hp 1–1 compared to polymeric Hp 2–1 and 2–2.

Cumulative glycosylation analyses obscured the Hp type-dependent differences in sialylation observed for specific glycosylation sites. This suggests that for the identification and quantification of the specific glycostructures, i.e. in biomarker research, studies should be performed at the level of the individual glycosylation sites.

Lastly, Hp glycosylation is known to be altered in many diseases. However, in most reports in which Hp glycosylation has been studied as

a biomarker, the effect of the Hp phenotype is completely ignored. Our study provides clear evidence that there are significant differences in glycosylation among the Hp phenotypes, even in the healthy population. Specifically, we observed most of the changes at the N184 and N241 in Hp type 1–1 compared to the other two types of Hp. Therefore, in Hp glycobiomarker discovery studies, we suggest considering the characterization of Hp phenotype, especially when the potential glyco-biomarkers are related to the N184 or N241 sites, in order to decrease the rate of reported false-positive and negative results.

Funding

Declaration of Competing Interest

The authors declare that they have no known competing financial interests or personal relationships that could have appeared to influence the work reported in this paper.
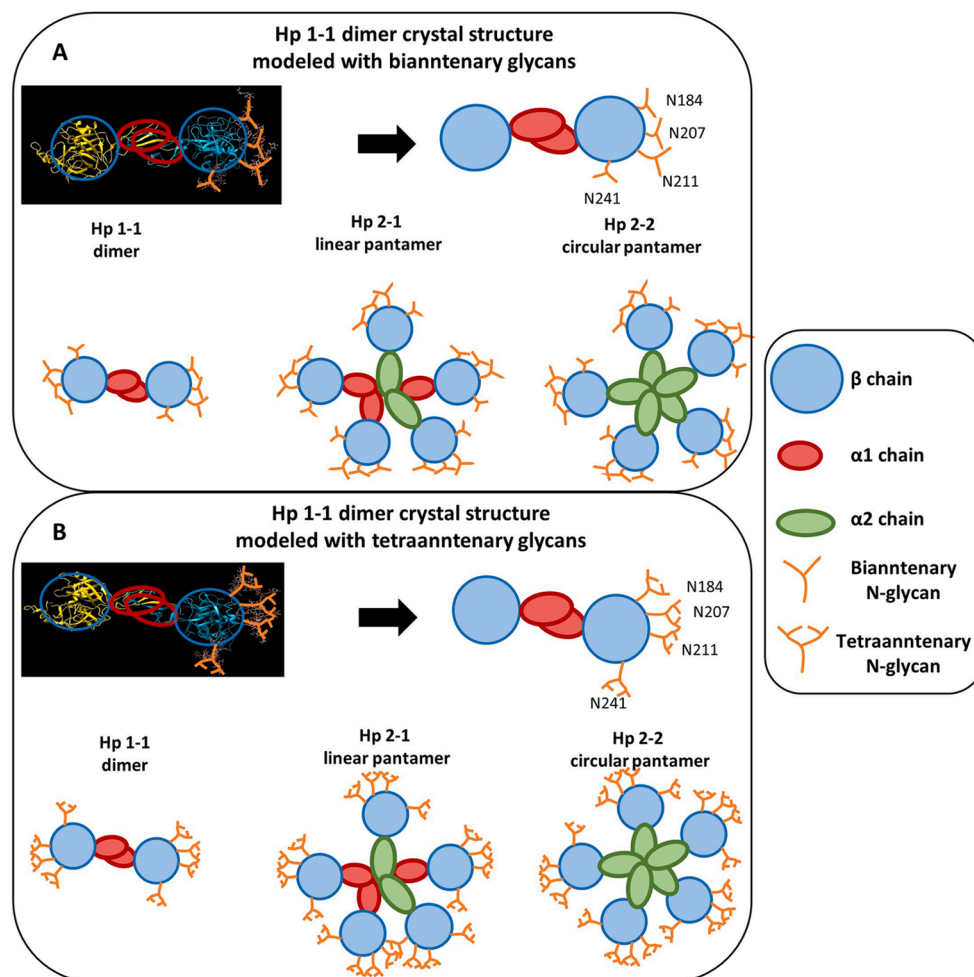
Fig. 6. Highly branched glycoforms introduce steric hindrance in Hp type 2–1 and 2–2 polymers. Using the crystal structure of Hp dimer, biantennary (A) and tetraantennary (B) glycans on N184, N207, N211, and N241 in Hp type 1–1 dimers, Hp type 2–1 linear pentamer and Hp type 2–2 circular pentamer, were modeled. Based on our data and the model, highly branched glycans introduce more steric hindrance in type 2–2 and type 2–1 compared to dimers of type 1–1.

Data availability

The dataset generated in this study containing all the identified and quantified glycopeptides in each sample and in different treatment conditions is summarized in Supplementary Tables 1 (no treatment condition), 2 (total neuraminidase treatment condition), 3 (2–3 neur-aminidase treatment condition) and 4 (Endo F3 treatment condition).

Acknowledgments

Appendix A.   Supplementary data

Supplementary data to this article can be found online at https://doi.org/10.1016/j.jmsacl.2022.07.001.

References

[1] S. Zhang, et al., Insights on N-glycosylation of human haptoglobin and its association with cancers, Glycobiology 26 (7) (2016) 684–692.

[2] J. D'Armiento, S.S. Dalal, K. Chada, Tissue, temporal and inducible expression pattern of haptoglobin in mice, Gene 195 (1) (1997) 19–27.

[3] F. Yang, et al., Pulmonary expression of the human haptoglobin gene, Am. J. Respir. Cell Mol. Biol. 23 (3) (2000) 277–282.

[4] Galicia G., et al., Haptoglobin Function and Regulation in Autoimmune Diseases, in Acute Phase Proteins - Regulation and Functions of Acute Phase Proteins, F. Veas, Editor.

[5] A.P. Levy, et al., Haptoglobin: Basic and Clinical Aspects, Antioxid. Redox Signal. 12 (2) (2009) 293–304.

[6] D.J. Schaer, et al., Haptoglobin, hemopexin, and related defense pathways-basic science, clinical perspectives, and drug development, Front Physiology 5 (2014) 415.

[7] M.R. Langlois, J.R. Delanghe, Biological and clinical significance of haptoglobin polymorphism in humans, Clin. Chem. 42 (10) (1996) 1589–1600.

[8] P.W. Buehler, et al., Haptoglobin preserves the CD163 hemoglobin scavenger pathway by shielding hemoglobin from peroxidative modification, Blood 113 (11) (2009) 2578–2586.

[9] M. Melamed-Frank, et al., Structure-function analysis of the antioxidant properties of haptoglobin, Blood 98 (13) (2001) 3693–3698.

[10] Y. Wang, et al., Haptoglobin, an inflammation-inducible plasma protein, Redox Rep. 6 (6) (2001) 379–385.

[11] J. Zhu, et al., Differential Quantitative Determination of Site-Specific Intact N-Glycopeptides in Serum Haptoglobin between Hepatocellular Carcinoma and Cirrhosis Using LC-EThcD-MS/MS, J. Proteome Res. 18 (1) (2019) 359–371.

[12] H. Asazawa, et al., Serum fucosylated haptoglobin in chronic liver diseases as a potential biomarker of hepatocellular carcinoma development, Clin. Chem. Lab. Med. 53 (1) (2015) 95–102.

[13] Y. Kamada, et al., Reevaluation of a lectin antibody ELISA kit for measuring fucosylated haptoglobin in various conditions, Clin. Chim. Acta 417 (2013) 48–53.

[14] K. Dalal, et al., Analysis of serum Haptoglobin using glycoproteomics and lectin immunoassay in liver diseases in Hepatitis B virus infection, Clin. Chim. Acta 495 (2019) 309–317.

[15] D. Ivanov, et al., Rapid Evaluation of the Extent of Haptoglobin Glycosylation Using Orthogonal Intact-Mass MS Approaches and Multivariate Analysis, Anal. Chem. 94 (12) (2022) 5140–5148.

[16] S. Tamara, V. Franc, A.J.R. Heck, A wealth of genotype-specific proteoforms fine-tunes hemoglobin scavenging by haptoglobin, Proc. Natl. Acad. Sci. USA 117 (27) (2020) 15554–15564.

[17] D. Wu, et al., N-glycan microheterogeneity regulates interactions of plasma proteins, Proc. Natl. Acad. Sci. USA 115 (35) (2018) 8763–8768.

[18] A. Sarrats, et al., Glycosylation of liver acute-phase proteins in pancreatic cancer and chronic pancreatitis, Proteomics Clin. Appl. 4 (4) (2010) 432–448.

[19] Z. Lin, et al., Mass spectrometric assay for analysis of haptoglobin fucosylation in pancreatic cancer, J. Proteome Res. 10 (5) (2011) 2602–2611.

[20] K. Morishita, et al., Haptoglobin phenotype is a critical factor in the use of fucosylated haptoglobin for pancreatic cancer diagnosis, Clin. Chim. Acta 487 (2018) 84–89.

[21] B. Paton, et al., Glycosylation Biomarkers Associated with Age-Related Diseases and Current Methods for Glycan Analysis, Int. J. Mol. Sci. 22 (11) (2021) 5788.

[22] J.N. Arnold, et al., Novel glycan biomarkers for the detection of lung cancer, J. Proteome Res. 10 (4) (2011) 1755–1764.

[23] Hoagland, L.F.M.4th, et al., Haptoglobin and posttranslational glycan-modified derivatives as serum biomarkers for the diagnosis of nonsmall cell lung cancer, Cancer 110 (10) (2007) 2260–2268.

[24] S.Y. Park, et al., α1-3/4 fucosylation at Asn 241 of β-haptoglobin is a novel marker for colon cancer: a combinatorial approach for development of glycan biomarkers, Int. J. Cancer 130 (10) (2012) 2366–2376.

[25] J. Wu, et al., Analysis of glycan variation on glycoproteins from serum by the reverse lectin-based ELISA assay, J. Proteome Res. 13 (4) (2014) 2197–2204.

[26] M. Ferens-Sieczkowska, M. Olczak, Carbohydrate structures of haptoglobin in sera of healthy people and a patient with congenital disorder of glycosylation, Z. Naturforsch., C: J. Biosci. 56 (1–2) (2001) 122–131.

[27] Scientific, T.F. *Western Blotting Using Polyvinylidene Difluoride (PVDF) Membranes.* Available from: https://www.thermofisher.com/de/de/home/references/protocols/proteins-expression-isolation-and-analysis/western-blot-protocol/western-blotting-using-polyvinylidene-difluoride-membranes.html.

[28] S. Neelamegham, et al., Updates to the Symbol Nomenclature for Glycans guidelines, Glycobiology 29 (9) (2019) 620–624.

[29] A. Varki, et al., Symbol Nomenclature for Graphical Representations of Glycans, Glycobiology 25 (12) (2015) 1323–1324.

[30] A. Ceroni, et al., GlycoWorkbench: A Tool for the Computer-Assisted Annotation of Mass Spectra of Glycans, J. Proteome Res. 7 (4) (2008) 1650–1659.

[31] M.K. Higgins, et al., Structure of the trypanosome haptoglobin-hemoglobin receptor and implications for nutrient uptake and innate immunity, Proc. Natl. Acad. Sci. U.S.A 110 (5) (2013) 1905–1910.

[32] A. Bohne-Lang, C.W. von der Lieth, GlyProt: in silico glycosylation of proteins, Nucleic Acids Res 33 (Web Server issue) (2005) W214–219.

[33] S. Tyanova, et al., The Perseus computational platform for comprehensive analysis of (prote)omics data, Nat. Methods 13 (9) (2016) 731–740.

[34] M. Nemansky, W.E.C.M. Schiphorst, D.H. Van den Eijnden, Branching and elongation with lactosaminoglycan chains of N-linked oligosaccharides result in a shift toward termination with α2→3-linked rather than with α2→6-linked sialic acid residues, FEBS Letts 363 (3) (1995) 280–284.

[35] Y.H. Lin, et al., Glycoproteogenomics: A Frequent Gene Polymorphism Affects the Glycosylation Pattern of the Human Serum Fetuin/α-2-HS-Glycoprotein, Mol. Cell. Proteomics 18 (8) (2019) 1479–1490.

[36] M. Larsson, T.-M. Cheng, C.-Y. Chen, S.J.T. Mao, *Unique Assembly Structure of Human Haptoglobin Phenotypes 1–1, 2–1, and 2–2 and a Predominant Hp 1 Allele Hypothesis*, in *Acute Phase Proteins*, S. Janciauskiene, Editor. (2013).

[37] C.A. Schaer, et al., Phenotype-specific recombinant haptoglobin polymers co-expressed with C1r-like protein as optimized hemoglobin-binding therapeutics, BMC Biotech. 18 (1) (2018) 15.

[38] A. Guillot, et al., Impact of sialic acids on the molecular dynamic of bi-antennary and tri-antennary glycans, Sci. Rep. 6 (1) (2016) 35666.

[39] *Essentials of Glycobiology, 2nd edition*, ed. Varki A., Cummings, R.D., Esko, J.D., Freeze, H.H., Stanley, P., Bertozzi, C.R., Hart, G.W., and Etzler, M.E. 2009.

[40] M. Lipiski, et al., Human Hp1-1 and Hp2-2 Phenotype-Specific Haptoglobin Therapeutics Are Both Effective In Vitro and in Guinea Pigs to Attenuate Hemoglobin Toxicity, Antioxid. Redox Signal. 19 (14) (2013) 1619–1633.

[41] R. Asleh, et al., Haptoglobin Genotype- and Diabetes-Dependent Differences in Iron-Mediated Oxidative Stress In Vitro and In Vivo, Circ. Res. 96 (4) (2005) 435–441.